

Supporting Information

Efficient Photocatalytic Water Reduction by a Cobalt(II) Tripodal Iminopyridine Complex

C.-F. Leung,^{a,*} S.-C. Cheng,^b Y. Yang,^a J. Xiang,^{a,c} S.-M. Yiu,^b C.-C. Ko,^{b,*} T.-C. Lau^b

^aDepartment of Science and Environmental Studies, The Education University of Hong Kong, 10 Lo Ping Road, Tai Po, Hong Kong, China.

^bDepartment of Chemistry, City University of Hong Kong, Tat Chee Avenue, Kowloon, Hong Kong, China.

^cDepartment of Chemical and Environmental Engineering, Yangtze University, Jingzhou, China

Table S1. Crystallographic data of **2**.

Formula	C ₂₄ H ₂₇ Cl ₂ CoN ₇ O ₈
FW	671.36
Crystal system	monoclinic
Space group	C12/c1
a, b, c/Å	27.9963(7), 10.5409(3), 19.1609(5)
α, β, γ/deg	90.0, 100.453(2), 90.0
Volume/Å ³	5560.7(3)
Z	8
D _{calc} /g cm ⁻³	1.604
μ(Cu Kα)/mm ⁻¹	7.150
F(000)	2760
Temperature/K	173(2)
λ/Å	1.54178
θ _{min} , θ _{max} /deg	71.84, 4.49
total, unique data	4272, 5357
R1(obsd/all)	0.0482/ 0.0652
wR2(obsd/all)	0.1281/ 0.1423
goodness-of-fit on F ²	1.044

Table S2. Selected bond distances (Å) and angles (°) of **2**.

Co(1)-N(1)	2.170(3)	N(2)-C(6)	1.259(5)
Co(1)-N(2)	2.119(3)	N(4)-C(14)	1.264(4)
Co(1)-N(3)	2.236(3)	N(6)-C(22)	1.265(5)
Co(1)-N(4)	2.113(3)	N(2)-C(7)	1.464(4)
Co(1)-N(5)	2.234(3)	N(4)-C(15)	1.461(4)
Co(1)-N(6)	2.103(3)	N(6)-C(23)	1.474(4)
N(4)-Co(1)-N(1)	163.65(11)	N(2)-Co(1)-N(1)	76.12(11)
N(2)-Co(1)-N(5)	168.15(11)	N(4)-Co(1)-N(3)	75.99(11)
N(6)-Co(1)-N(3)	162.60(11)	N(6)-Co(1)-N(5)	75.23(11)

Table S3. Selected bond distances (Å) in the optimized structures of **1** at various oxidation and spin states

Oxidation State	0	1	2 (high spin)	2 (low spin)	3
Co-N(imine)	2.0991	2.1044	2.1398	2.0044	1.9136
Co-N(pyridine)	2.1992	2.2092	2.2124	2.1000	1.9775

Table S4. Selected bond distances (Å) in the optimized structures of **2** at various oxidation and spin states

Oxidation State	0	1	2 (high spin)	2 (low spin)	3
Co-N(tren)	3.3073	3.2703	2.8131	3.3576	3.4542
Co-N(imine)	2.1181	2.1164	2.1220	2.0477	1.9490
Co-N(pyridine)	2.1835	2.1795	2.2373	2.0740	1.9565

Table S5. Selected bond distances (Å) in the optimized structures of **1** in the Co^I state and Co^I state with an added proton.

	[Co(tachpy ₃)] ⁺	[Co(tachpy ₃ -H)] ²⁺
Co-N(imine) [average distance]	2.104	2.044
Co-N(pyridine) [average distance]	2.209	2.209
Co-N(pyridine-H)		3.210
Co-H(pyridine-H)		2.584

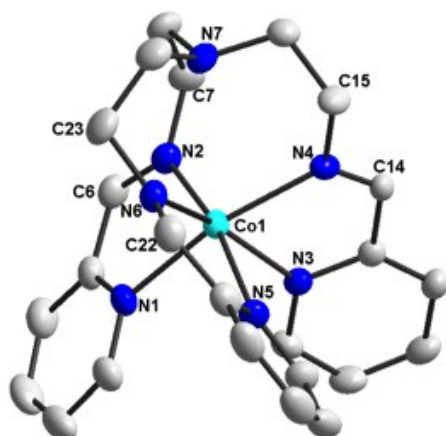


Figure S1. ORTEP drawing of the cation of **1**. Thermal ellipsoids are drawn at 50% probability and hydrogen atoms are omitted for clarity.

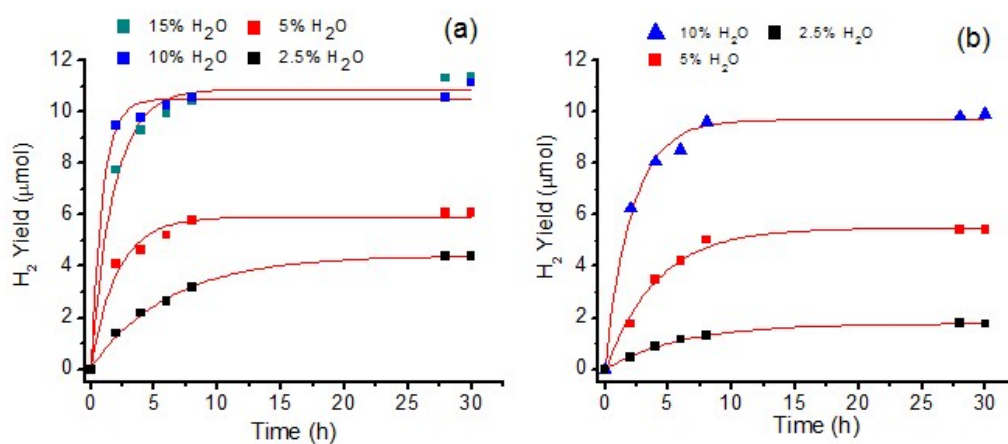


Figure S2. Photocatalytic H₂ generation of (a) **1** (1 μM) and (b) **2** (1 μM) at varied concentrations of water in acetonitrile; [IrPS⁺] = 0.2 mM and [TEA] = 0.2 M; λ > 420nm.

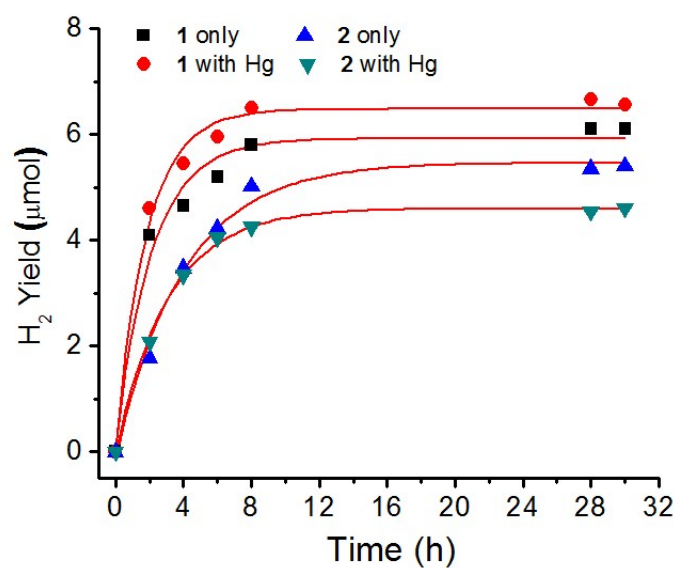


Figure S3. Effect of Hg^0 (0.5 mL) addition on the photocatalytic H_2 generation by **1** and **2** (1 μM) in aqueous acetonitrile (5% v/v); $[\text{IrPS}^+] = 0.2 \text{ mM}$ and $[\text{TEA}] = 0.2 \text{ M}$; $\lambda > 420\text{nm}$.

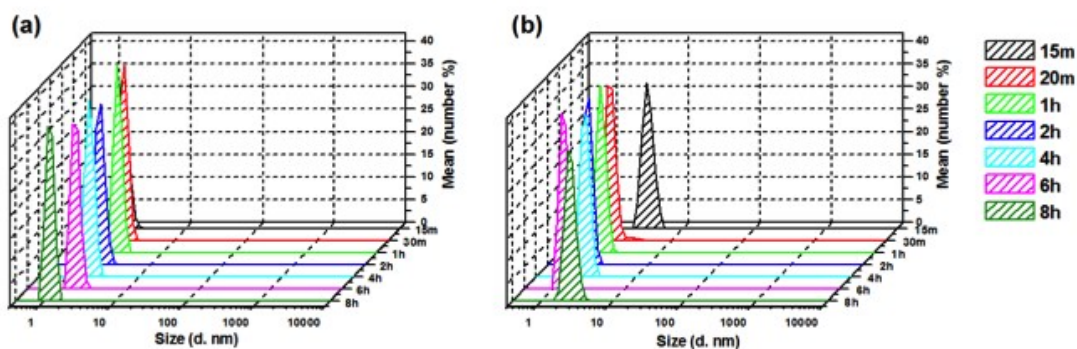


Figure S4. Temporal distribution of particle size obtained by dynamic light scattering for a) **1** and b) **2** (50 M) in 10% aqueous acetonitrile (v/v) containing 0.2mM IrPS^+ and 0.2 M TEA during the first 8h of photolysis.

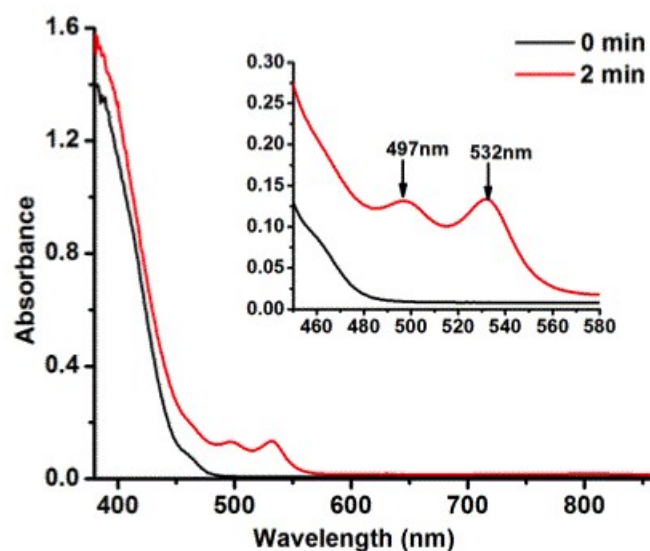


Figure S5. Spectral change of IrPS⁺ (0.25 mM) in the presence of 6.25 mM TEOA in acetonitrile upon broadband irradiation ($\lambda > 420$ nm) for 2 min. Inset: absorption bands at 463, 497 and 532 nm.

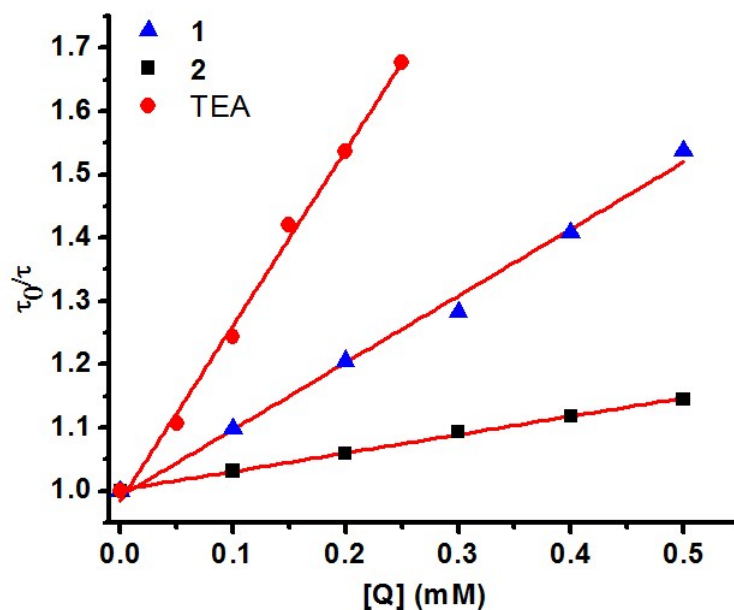


Figure S6. Stern-Volmer plots for the reductive quenching of IrPS⁺ (0.05 mM) in acetonitrile with **1** [slope = 291 ± 6 ; y-intercept = 1.002 ± 0.002] ($k_q = 1.32 \times 10^8$), **2** [slope = 1056 ± 40 ; y-intercept = 0.991 ± 0.012] ($k_q = 4.79 \times 10^8$) and **TEA** [slope = 2768 ± 84 ; y-intercept = 0.984 ± 0.013] ($k_q = 1.15 \times 10^9$).

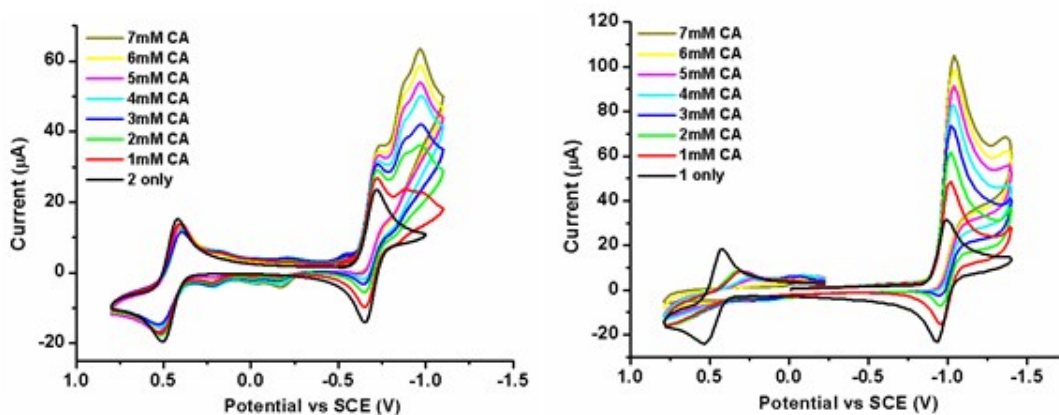


Figure S7. CVs of 1mM of **1** (left) and **2** (right) in the presence of varied amount (1–7mM) of aqueous citric acid (0.7M) in 0.1M $n\text{Bu}_4\text{NPF}_6$ acetonitrile solution. Scan rate = 100 mVs^{-1} .

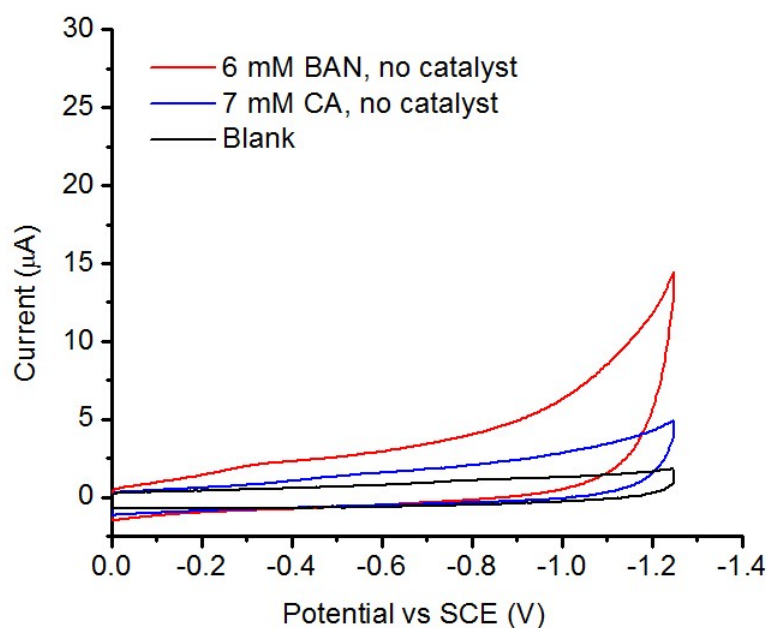


Figure S8. CVs of 6mM bromocyclohexylamine triflate (BAN) and 7mM aqueous citric acid (CA) in 0.1M $n\text{Bu}_4\text{NPF}_6$ acetonitrile solution in the absence of catalysts. Scan rate = 100 mVs^{-1} .

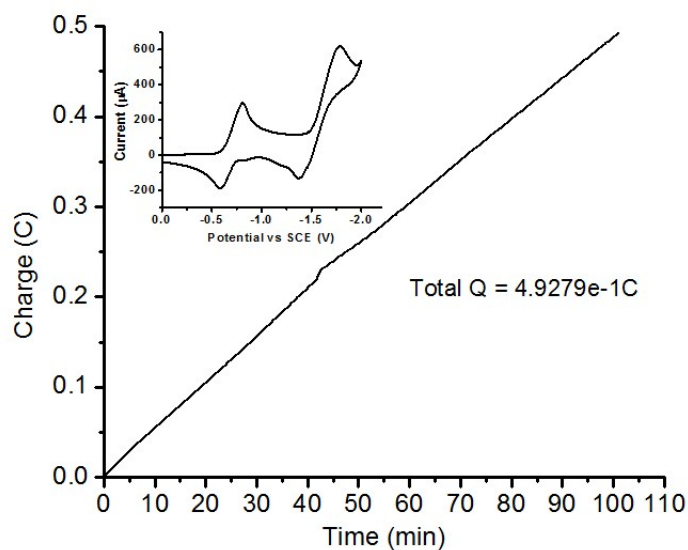


Figure S9. Controlled potential electrolysis of **1** (1mM) in 0.1M $n\text{Bu}_4\text{NPF}_6$ acetonitrile solution at -1V vs SCE using an iTO plate working electrode, Pt counter electrode and SCE reference electrode. Inset: CV of **1** obtained using the same cell configuration.

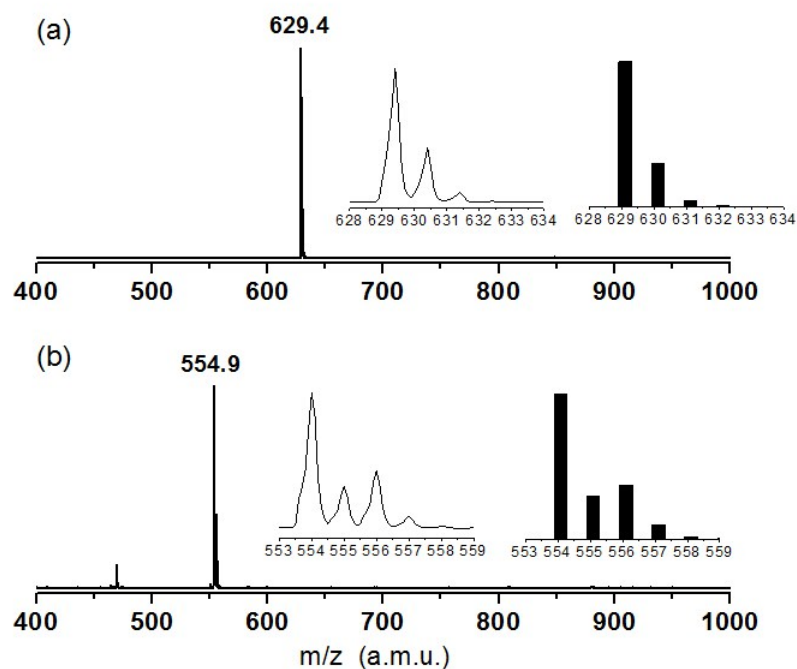


Figure S10. ESI-MS of the diluted ($\times 10$) acetonitrile solution of (a) 1mM solution of **1** in 0.1M $n\text{Bu}_4\text{NPF}_6$ acetonitrile electrolyzed at -1V vs SCE using an iTO plate working electrode; (b) **1** in acetonitrile solution.

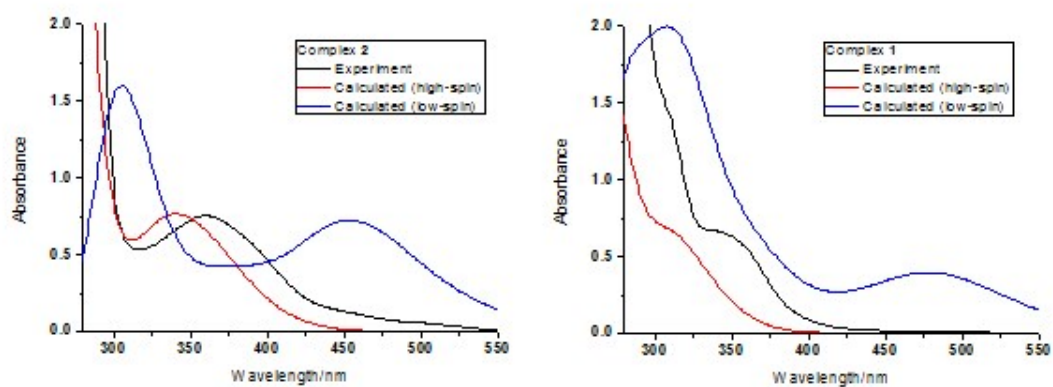


Figure S11. Simulated and experimental (acetonitrile) UV/Vis spectra of **1** and **2**.

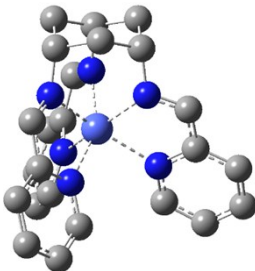
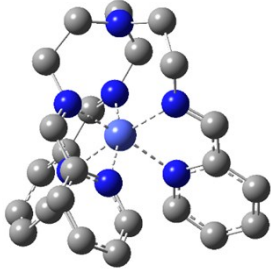
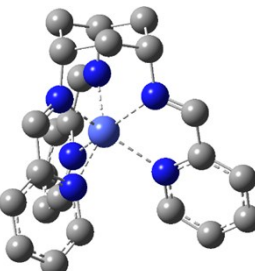
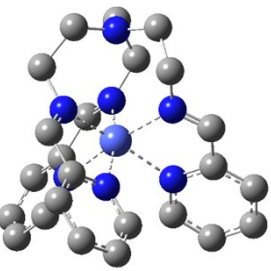
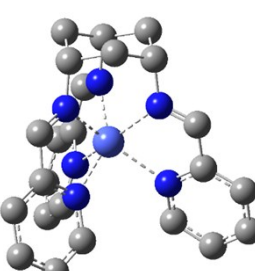
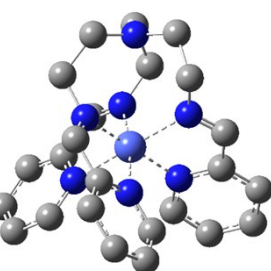
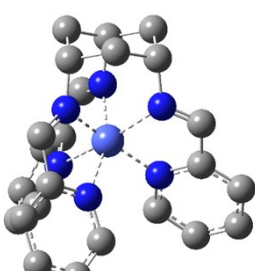
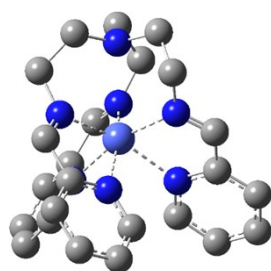
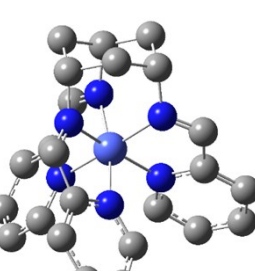
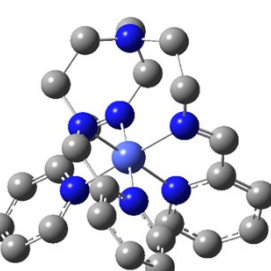
Oxidation State	1 [Co(tachpy ₃)] ⁿ⁺	2 [Co(trenpy ₃)] ⁿ⁺
0		
1		
2 (high spin)		
2 (low spin)		
3		

Figure S12. Optimized structures of **1** and **2** at various oxidation and spin

states.

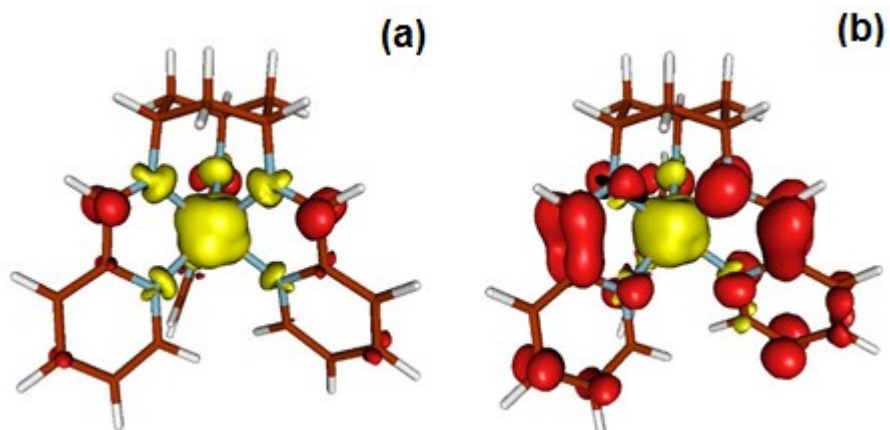


Figure S13. The calculated spin densities of the optimized structures of (a) the singly positive charged Co^{I} state and (b) the doubly reduced $[\text{Co}^{\text{I}}(\text{L}\cdot)]^0$ state of **1**.